

# Food & Function

Accepted Manuscript



This is an *Accepted Manuscript*, which has been through the Royal Society of Chemistry peer review process and has been accepted for publication.

*Accepted Manuscripts* are published online shortly after acceptance, before technical editing, formatting and proof reading. Using this free service, authors can make their results available to the community, in citable form, before we publish the edited article. We will replace this *Accepted Manuscript* with the edited and formatted *Advance Article* as soon as it is available.

You can find more information about *Accepted Manuscripts* in the [Information for Authors](#).

Please note that technical editing may introduce minor changes to the text and/or graphics, which may alter content. The journal's standard [Terms & Conditions](#) and the [Ethical guidelines](#) still apply. In no event shall the Royal Society of Chemistry be held responsible for any errors or omissions in this *Accepted Manuscript* or any consequences arising from the use of any information it contains.

**Tartary Buckwheat Flavonoids protect hepatic cells against high glucose-induced oxidative stress and insulin resistance via MAPKs signaling pathways**

Yuanyuan Hu<sup>1,†</sup>, Zuoxu Hou<sup>2,†</sup>, Dongyang Liu<sup>3</sup>, Xingbin Yang<sup>1,\*</sup>

<sup>1</sup>College of Food Engineering and Nutritional Science, Shaanxi Normal University, Xi'an 710062, China

<sup>2</sup>Department of Aerospace Medicine, Fourth Military Medical University, Xi'an 710032, China

<sup>3</sup>The first brigade of cadets, Fourth Military Medical University, Xi'an 710032, China

†These two authors contributed equally to this study.

\*Corresponding author: Tel.: +86-29-85310517; fax: +86-29-85310517

E-mail address: xbyang@snnu.edu.cn (X.B. Yang)

## 1 **Abstract**

2 Oxidative stress attributes a crucial role in chronic complication of diabetes. In this study, the  
3 protective effect of purified tartary buckwheat flavonoids fraction (TBF) against oxidative stress  
4 induced by a high-glucose challenge, which causes insulin resistance, was investigated on  
5 hepatic HepG2 cells. Oxidative status, phosphorylated mitogen-activated protein kinases  
6 (MAPKs), nuclear factor E2 related factor 2 (Nrf2) and p-(Ser307)-IRS-1 expression, and  
7 glucose uptake were evaluated. Results suggest that treatment of HepG2 cells with TBF alone  
8 improved glucose uptake and antioxidant enzymes, and activated Nrf2, and attenuated the IRS-1  
9 Ser307 phosphorylation, and enhanced total levels of IRS-1. Furthermore, the high  
10 glucose-induced changes in antioxidant defences, Nrf2, p-MAPKs, p-IRS1 Ser307, and IRS-1  
11 levels, and glucose uptake were also significantly inhibited by pre-treatment with TBF.  
12 Interestingly, the selective MAPK inhibitors significantly enhanced the TBF-mediated  
13 protection by inducing changes in redox status, glucose uptake, p-(Ser307) and total IRS-1  
14 levels. This report firstly showed that TBF could recover redox status of insulin-resistant HepG2  
15 cells, suggesting that TBF significantly protected the cells against high glucose-induced  
16 oxidative insult, and these beneficial effects of TBF on redox balance and insulin resistance  
17 were mediated by targeting MAPKs.

18 **Keywords:** Type 2 diabetes mellitus, Oxidative stress, Tartary buckwheat flavonoids, HepG2  
19 cells, Antioxidant defences

## 20 Introduction

21 Type 2 diabetes mellitus (T2DM), a complex metabolic disorder, is the most serious and  
22 common cause of morbidity and mortality in modern civilization.<sup>1</sup> Several lines of evidence  
23 suggest that oxidative stress plays a main role in the pathogenesis of T2DM,<sup>2,3</sup> where there is a  
24 miss-regulation of the glucose homeostasis and the insulin pathway, leading to the decrease in  
25 the levels of in vivo antioxidants because of the oxidative stress induced by the  
26 hyper-glycaemia.<sup>4-7</sup> However, the modulation of Phase I [glutathione reductase (GR),  
27 glutathione peroxidase (GPx) and catalase (CAT)] and Phase II [glutathione S-transferase (GST)]  
28 enzymes, and glutathione (GSH) levels plays a primary role in the balance of the redox status  
29 through the reduction of reactive oxygen species (ROS).<sup>8,9</sup> In this line, the redox-sensitive  
30 transcription factor nuclear factor E2 related factor 2 (Nrf2), which is a primary transcription  
31 factor responsible for initiating the antioxidative response to reactive oxygen species, could be  
32 regulated by dietary flavonoids,<sup>10,11</sup> and its primary control of function lies on its subcellular  
33 distribution and/or phosphorylation.<sup>12,13</sup> Moreover, the three major mitogen-activated protein  
34 kinases (MAPKs) signaling pathways, including extracellular signal-related protein kinases  
35 (ERK1/2), c-Jun NH<sub>2</sub>-terminal protein kinases (JNKs) and p38,<sup>14</sup> were regulated by oxidative  
36 stress and insulin resistance,<sup>13</sup> and could also be modulated by dietary flavanols,<sup>15,16</sup> and  
37 ERK1/2 and p38 have been demonstrated to be main regulators of Nrf2.<sup>13</sup>

38 Extensive evidence has shown that compounds with strong antioxidant property exert  
39 beneficial effects against hyperglycaemia, insulin resistance and oxidative stress,<sup>17,18</sup> which can

40 be served as a promising approach in the prevention and/or treatment of T2DM.<sup>3,19</sup> Tartary  
41 buckwheat (*Fagopyrum tataricum* L., Gaench), a very important edible and medicinal plant in  
42 China, have demonstrated to be associated with a lower prevalence of hyperglycemia and  
43 improved glucose tolerance in people with diabetes.<sup>20-22</sup> Its beneficial health effects are bound  
44 up with its high content of flavonoids, especially rutin and quercetin.<sup>23,24</sup> Additionally, rutin, the  
45 major ingredient of buckwheat,<sup>25</sup> has recently been validated as novel strategies for the  
46 prevention of type 2 diabetes since it exerts significant anti-diabetic activity by protecting the  
47 integrity of pancreatic  $\beta$  cells, restoring the depleted liver antioxidant status, increasing glucose  
48 transporter 4 (GLUT4) translocation and reducing plasma glucose in type 2 diabetic rats.<sup>26-29</sup>  
49 Quercetin, as the aglycon of rutin, has been demonstrated to exhibit beneficial effects in diabetes  
50 mellitus by inhibiting hepatic glucose production, enhancing glucose uptake, potentiating insulin  
51 secretion, as well as protecting INS-1 pancreatic  $\beta$  cells against oxidative stress via the ERK1/2  
52 pathway.<sup>19,30-33</sup> All the above indicates that rutin and quercetin are interesting in health  
53 protective benefits on T2DM, including insulinomimetic and antioxidant effects. Thereby, it  
54 could be hypothesized that tartary buckwheat flavonoids could exert an antidiabetic effect by  
55 reducing or even suppressing the oxidative stress of T2DM through the modulation of the  
56 cellular antioxidant defences and close-related key proteins for that response. Nevertheless, the  
57 enzymatic response of the antioxidant defences and the role of Nrf2 during insulin resistance in  
58 T2DM are still remaining unclear.<sup>16</sup> In this regard, the protective effects of tartary buckwheat  
59 flavonoids on the response of the antioxidant defence molecular mechanism during insulin

60 resistance in the liver was firstly studied in terms of antioxidant defences, Nrf2 and regulation  
61 by MAPKs.

62 The aim of the study was therefore to investigate the protective effects of TBF against the  
63 oxidative stress in a well-established model of insulin resistant HepG2 cells induced by a  
64 high-glucose challenge. Furthermore, we also aimed to determine the mechanisms underlying  
65 the process by evaluating the markers of oxidative damage, antioxidant defences and related  
66 signals, as well as stress-related signalling pathways and keys features of insulin resistance. This  
67 study provided an important clue for substantiating dietary and therapeutic use of tartary  
68 buckwheat to prevent the oxidative stress related complication in type 2 diabetes mellitus.

69

## 70 **Materials and method**

### 71 **Materials and reagents**

72 Tartary buckwheat powder was obtained from Liangshan Qiongzhu Tartary Buckwheat  
73 Products Co. Ltd. (Sichuan, China). Dulbecco's modified Eagle's medium (DMEM) and fetal  
74 bovine serum (FBS) were purchased from Gibco Laboratories, Inc. (Grand Island, NY, USA).  
75 3-(4,5-Dimethylthiazol-2-yl)-2,5-diphenyltetrazoliumbromide (MTT), D-glucose, gentamicin,  
76 penicillin G, streptomycin, dimethyl sulfoxide (DMSO) and *o*-phthaldehyde (OPT) were  
77 purchased from Sigma Co. (St. Louis, MO, USA). 2,7-Dichlorodihydrofluorescein diacetate  
78 (DCF-DA) was from Molecular Probes (Carlsbad, CA, USA). The assay kits for GSH, GR, GPx,  
79 CAT and GST were obtained from Beyotime Co. (Jiangsu, China).

80 2-(7-Nitrobenz-2-oxa-1,3-diazol-4-yl) amino-2-deoxy-D-glucose (2-NBDG) was purchased  
81 from Molecular Probe (Invitrogen Life Technologies, Carlsbad, CA, USA). Antibodies against  
82 ERK1/2, phospho-ERK1/2 (p-ERK) (Thr202/Thy204), JNK1/2, phospho-JNK1/2 (p-JNK)  
83 (Thr183/Tyr185), p38 MAPK, phospho-p38 (p-p38) (Thr180/Tyr182), phospho-(Ser307)-IRS-1  
84 and horseradish-peroxidase (HRP)-conjugated secondary antibodies were obtained from Cell  
85 Signaling Technology, Inc. (Cell Signaling Technology, USA). Anti-Nrf2,  $\beta$ -actin and anti-lamin  
86 B1 were purchased from Santa Cruz Biotechnology Inc. (Santa Cruz, CA, USA). The ERK  
87 inhibitor PD98059, p38 MAPK inhibitor SB203580 and JNK inhibitor SP600125 were obtained  
88 from Calbiochem (San Diego, CA, USA). Deionized water was prepared using a Millipore Milli  
89 Q-Plus system (Millipore, Bedford, MA, USA). All other chemicals made in China were of the  
90 highest grade available.

#### 91 **Extraction and purification of tartary buckwheat flavonoids**

92 Flavonoids fraction of tartary buckwheat was extracted by methanol-water (75:25, v/v) with  
93 reflux for 2 h, and repeated three times.<sup>34</sup> The combined extracts were centrifuged (10 min,  
94 3,000 g), and concentrated at 60 °C under vacuum, and then freeze-dried. The dry powder was  
95 diluted by deionized water, and then passed through the glass columns ( $\Phi$  12 mm  $\times$  500 mm)  
96 wet-packed with AB-8 resin to purify at the flow rate of 1.5 mL/min. After reaching adsorptive  
97 saturation, the column was firstly washed by deionized water, and then eluted by 60% ethanol.  
98 The eluate was collected, followed by freeze-drying, and then obtained the purified tartary  
99 buckwheat flavonoid fraction (TBF). A detailed description of this TBF has been previously

100 published.<sup>34</sup> Accordingly, the amount of rutin and quercetin present in the TBF were 536.2 mg/g  
101 and 371.6 mg/g, respectively, accounting for up to 90.8% of TBF (determined by HPLC).<sup>34</sup>

## 102 **Cell culture and treatments**

103 Human hepatic cell line (HepG2), a reliable model, is widely used for biochemical and  
104 nutritional studies, where many antioxidants and conditions can be assayed with minor  
105 inter-assay variations, and variations of responses to different conditions are more easily  
106 detected.<sup>35,36</sup> In the present study, the HepG2 cells were obtained from the Fourth Military  
107 Medical University (Xian, China) and cultured in DMEM-F12 medium, supplemented with  
108 2.5% FBS and 50 mg/L antibiotics (gentamicin, penicillin, and streptomycin). The cells were  
109 maintained at 37 °C in a humidified atmosphere of 5% CO<sub>2</sub>. One day after plating, the medium  
110 was changed to DMEM containing 5.5 mM D-glucose, 2 mM glutamine and fetal bovine serum,  
111 and the culture was continued. Cells were grown upon reaching 70% confluence and then  
112 pre-incubated in serum-free medium for 24 h before treatments.

113 High dose of glucose was demonstrated to induce insulin resistance, evoked an imbalance of  
114 cell redox status, and also induced a response to stress in HepG2 by activating Nrf2 and MAPK  
115 pathways.<sup>16</sup> In our study, the dosage of 30 mM glucose was selected to induce oxidative stress  
116 and insulin resistance. According to the previously reports,<sup>37,38</sup> the cells were exposed to 100 nM  
117 insulin for 10 min after 24 h of incubation with 30 mM D-glucose in serum-free media, and then  
118 harvested and tested for ROS production, GSH and carbonyl content, and enzymatic activities  
119 (GPx, GR, CAT and GST).



120 To evaluate the protective effect of TBF against high-glucose challenge. TBF was dissolved  
121 in DMSO to make a stock solution of 50 mg/mL and further diluted to final concentrations of 25,  
122 50, and 100 µg/mL with serum-free culture medium. The TBF doses were selected based on our  
123 previous experiments, since these realistic concentrations were the lowest doses tested that did  
124 not induce cellular damage, exhibited a prominent effect on the the ROS and GSH contents.<sup>39</sup>  
125 The final concentration of DMSO in culture medium was maintained at 0.05%.<sup>40</sup> Different  
126 concentrations of TBF were added to the cells for 24 h, and then, the medium was discarded and  
127 fresh medium containing 30 mM glucose was added for additional 24 h. Later, the cells were  
128 exposed to 100 nM insulin for 10 min to test the response to insulin and then harvested. In the  
129 experiments with the pharmacological inhibitors, cells were pre-incubated with 50 µM PD98059,  
130 10 µM SB203580 or 40 µM SP600125 for 1 h prior to high-glucose challenge. The  
131 concentrations of the inhibitors employed have been selected according to the previously used  
132 doses in HepG2 cells.<sup>16,18</sup>

### 133 **Assessment of cell viability and proliferation**

134 Cell viability was determined by using the MTT assay.<sup>41</sup> HepG2 cells were seeded at a density  
135 of  $1 \times 10^4$  cells/mL in 96-well polystyrene culture plates at 37 °C with 5% (v/v) CO<sub>2</sub> for one day.  
136 After 24 h of incubation, 100 µL of the medium was removed from each well, and 100 µL of  
137 different concentrations of TBF (0, 25, 50, 100 µg/mL) were added and incubated for 24 h. Then  
138 100 µL of 0.5% (w/v) MTT in PBS solution was added to each well and incubated for an  
139 additional 4 h at 37 °C in a CO<sub>2</sub> incubator. Then MTT-containing media were removed, and 10%

140 SDS in DMSO was added to each well and the absorbance at 490 nm of solubilized MTT  
141 formazan products was measured using a micro-plate reader (Bio-Rad Laboratories Ltd., China).

142 For cell proliferation assay, a colorimetric bromodeoxyuridine (BrdU) Cell Proliferation  
143 ELISA Kit (Abcam, Cambridge, UK) was used.<sup>15,42</sup> HepG2 cells were seeded in 96-well  
144 polystyrene culture plates at a seeding density of  $10^4$  cells per well counted in a Neubauer  
145 chamber. After 20 h of grown, HepG2 cells were either left untreated (control) or exposed to a  
146 range of concentrations (0-100  $\mu\text{g}/\text{mL}$ ) for 24 h. BrdU was added 4 hours before the end of the  
147 incubation period. Cells were then fixed, DNA was denatured, and BrdU content was assessed  
148 using a monoclonal anti-BrdU antibody following the manufacturer's instructions. Then the  
149 immune complexes were quantified by measuring the absorbance at 620 nm in a micro-plate  
150 reader.

#### 151 **Detection of ROS production**

152 Cellular ROS were measured by the DCFH assay.<sup>42</sup> This dye is a stable nonpolar compound  
153 that diffuses readily into cells and yields DCFH. Intracellular ROS in the presence of peroxidase  
154 changes DCFH to the highly fluorescent compound DCF. Thus, the fluorescent intensity is  
155 proportional to the amount of ROS produced by the cells. For the assay, the cells were plated in  
156 24-well multi-wells at a rate of  $2 \times 10^5$  cells per well and changed to FBS-free medium or the  
157 different TBF concentrations the day after. Twenty hours later, 5  $\mu\text{M}$  DCFH was added to the  
158 wells for 30 min at 37 °C. Then, cells were washed twice with PBS, lysed in cell lysates, and  
159 centrifuged at 15,000 g for 10 min at 4 °C. The DCF fluorescence intensity of the supernatant

160 was measured via a fluorescence microplate reader at 485 nm excitation and 535 nm emission  
161 (Molecular Devices Co., Sunnyvale, CA). Cellular ROS levels were expressed as relative DCF  
162 fluorescence per microgram of protein. This parameter gives a very good evaluation of the  
163 degree of cellular oxidative stress.

#### 164 **Measurement of GSH**

165 The content of GSH was quantified by Hissin and Hilf fluorimetric assay.<sup>43</sup> The method is  
166 based on the reaction of GSH with *o*-phthaldehyde (OPT) at pH 8.0. After the different  
167 treatments, the culture medium was removed and cells ( $4 \times 10^6$ ) were detached and  
168 homogenized by ultrasound with 5% trichloroacetic acid containing 2 mM EDTA. Following  
169 centrifugation of cells for 30 min at 1,000 g, 50  $\mu$ L of the clear supernatant was transferred to a  
170 96 multi-well plate for the assay. Fluorescence was measured at excitation wavelength of 340  
171 nm and emission wavelength of 460 nm. The results of samples were referred to those of a  
172 standard curve of GSH.

#### 173 **Measurement of carbonyl groups**

174 Protein oxidation of cells was measured as carbonyl groups content according to a published  
175 method.<sup>44</sup> Treated cells ( $4 \times 10^6$ ) were collected in PBS and centrifuged at 300 g for 5 min to  
176 pellet cells. Then, cells were lysed with cell lysis buffer (Beyotime Institute of Biotechnology,  
177 Jiangsu, China), and centrifuged at 12,000 g for 20 min at 4 °C. Absorbance was measured at  
178 360 nm and carbonyl content was expressed as nmol/mg protein using an extinction coefficient  
179 of 22 000 nmol/L/cm. Protein was measured by the Bradford reagent.

**180 Measurement of GPx, GR, CAT and GST activities**

181 Treated cells ( $4 \times 10^6$ ) were collected in PBS and centrifuged at 300 g for 5 min to pellet cells  
182 to assay the enzymatic activities. Cell pellets were resuspended in 20 mM Tris containing 5 mM  
183 EDTA and 0.5 mM mercaptoethanol, sonicated and centrifuged at 3,000 g for 15 min, then the  
184 supernatants were collected and stored at  $-20\text{ }^\circ\text{C}$  until biochemical analysis. GPx activity was  
185 assayed using  $\text{H}_2\text{O}_2$  and NADPH as substrates. The conversion of NADPH to  $\text{NADP}^+$  was  
186 observed by recording the changes in absorption intensity at 340 nm.<sup>45</sup> GR activity was  
187 determined by following the decrease in absorbance due to the oxidation of NADPH utilized in  
188 the reduction of oxidized glutathione.<sup>46</sup> CAT activity was determined by the decomposition of  
189  $\text{H}_2\text{O}_2$  as a decrease in absorbance at 240 nm.<sup>47</sup> GST activity was analysed by a commercial  
190 activity assay kit.<sup>48</sup> The sample was mixed with  $\text{KH}_2\text{PO}_4$  buffer, EDTA, CDNB and GSH. The  
191 reaction was carried out at  $37\text{ }^\circ\text{C}$  and monitored spectrophotometrically at 340 nm for 5 min.

**192 Preparation of total and nuclear cell lysates**

193 Cells were seeded at a density of  $1 \times 10^6$  cells/mL in 60 mm polystyrene culture dishes at  
194  $37\text{ }^\circ\text{C}$  with 5% (v/v)  $\text{CO}_2$  for 24 h, and then cells were incubated with TBF for 24 h prior to 24-h  
195 glucose (Gluc) challenge and further exposed to 100 nM (Ins) for 10 min. After treatments,  
196 HepG2 cells were washed twice with PBS (pH 7.4) and lysed in lysis buffer (Beyotime Institute  
197 of Biotechnology, Jiangsu, China) containing 1% phenylmethylsulfonyl fluoride (PMSF) and 20  
198 mM NaF for 10 min on ice to detect total Nrf2, ERK, p-ERK, JNK, p-JNK, p38, p-p38 and  
199 p-(Ser307)-IRS-1. The lysed cells were removed from the culture dish by gentle scraping with a

200 rubber policeman and transferred to a microcentrifuge tube. To analyse nuclear Nrf2, cells were  
201 lysed with nuclear extraction reagent (Xianfeng Biotechnology, Xian, China). Samples were  
202 centrifuged for 20 min at 4 °C at 12,000 g. The supernatant fractions were collected, and  
203 aliquoted and stored at -80 °C until used for Western blot analyses. Protein concentrations were  
204 determined with a BCA protein assay kit (Beyotime, China).

### 205 **Western blot analysis**

206 After boiled with loading buffer for 10 min at 100 °C, proteins (100 µg) were separated by  
207 electrophoresis on SDS-PAGE and transferred to polyvinylidene difluoride membranes (PVDF)  
208 (0.45 µm, Millipore) using a semi-dry transfer apparatus (Bio-Rad, Shanghai, China). After  
209 blocked with 5% milk for 30 min at room temperature, membranes were incubated at 4 °C  
210 overnight with appropriate primary antibodies, followed by incubation with the corresponding  
211 horseradish peroxidase (HRP)-conjugated secondary antibodies at 25 °C for 2 h. Blots were  
212 detected by enhanced chemiluminescent (ECL) reagent (Pioneer Technology, USA).  
213 Normalization of Western blot was ensured by  $\beta$ -actin or lamin B1 for nuclear protein extracts,  
214 and band quantification was analyzed using Quantity One System (Bio-Rad, Richmond, CA,  
215 USA).

### 216 **Glucose uptake assay**

217 Cellular glucose uptake was assessed using the fluorescent glucose analog, 2-NBDG.<sup>5,28</sup>  
218 Briefly, cells were plated in 24-well plates ( $2 \times 10^5$  cells per well counted in a Neubauer  
219 chamber) and after the treatments, 2-NBDG was added at 10 µM final concentration for 1 h at

220 37 °C. Then, cells were washed twice with PBS, serum-free medium was added and  
221 fluorescence intensity was immediately measured in a micro-plate reader at an excitation  
222 wavelength of 485 nm and an emission wavelength of 530 nm. After being taken by the cells,  
223 2-NBDG was converted to a non-fluorescent derivative (2-NBDG metabolite). A fair estimation  
224 of the overall glucose uptake was obtained by quantifying the fluorescence.

### 225 **Statistical analysis**

226 All experiments were performed 3 times, and the data are presented as the mean  $\pm$  standard  
227 error (SE). Statistical comparisons were made using one-way ANOVA, followed by  
228 Bonferroni's correction if ANOVAs revealed statistical significances. The  $p$ -value  $< 0.05$  was  
229 considered to be statistically significant.

230

## 231 **Results**

### 232 **Cell viability and proliferation**

233 In order to investigate the potential effects of TBF on cell viability and cell proliferation in  
234 HepG2 cells, the cells were cultured with different concentrations (0-100  $\mu\text{g/mL}$ , respectively)  
235 for 24 h. As presented in Table 1, treatment of HepG2 cells with TBF up to 100  $\mu\text{g/mL}$  for 24 h  
236 did not evoke any changes in cell viability, as determined by the MTT assay, indicating that the  
237 concentrations selected for the study did not induce cellular damage during the period of  
238 incubation. Similarly, treatment with TBF had no significant impact on cell growth as assessed  
239 by a BrdU incorporation assay ( $p > 0.05$ ), indicating no impairment of cell proliferative

240 machinery and preservation of a regular cell cycle.

#### 241 **Effect of TBF on high glucose-induced oxidative stress**

242 To test the long-term protective effect of TBF on cultured HepG2 cells submitted to oxidative  
243 stress, the cells were pre-treated for 24 h with different concentrations of TBF prior to 24 h of 30  
244 mM glucose treatment followed by a 10 min chase with 100 nM insulin, and then, parameters  
245 related to redox status and antioxidant response were evaluated. As illustrated in Fig. 1, high  
246 glucose increased ROS and carbonyl groups levels, and decreased the GSH content when  
247 compared to control cells. However, treatment with TBF (100 µg/mL) alone significantly  
248 decreased the ROS production, and increased the GSH content ( $p < 0.05$ ), while did not alter the  
249 content of tested protein carbonyl. Interestingly, under high-glucose conditions, pre-treatment of  
250 HepG2 cells with TBF prevented the GSH depletion and reversed the increases of ROS and  
251 carbonyl groups induced by the high glucose in a dose-dependent manner (Fig. 1). Besides, both  
252 high glucose and TBF alone increased the GPx and GR activities when compared to control cells,  
253 while CAT and GST activities did not altered (Fig. 2). Additionally, GPx activity was restored to  
254 control levels by pre-treatment with all doses of TBF under high glucose conditions, and GR  
255 activity was restored to control levels by pre-treatment with TBF (25 and 50 µg/mL) under high  
256 glucose conditions, while CAT and GST activities remained unchanged after all incubations (Fig.  
257 2). It was also found that when cells were exposed to 100 µg/mL TBF alone, ROS production  
258 was reduced to a minimum level, and the GSH content, GPx and GR activities reached their  
259 maximum levels, showing the best effects compared with treating other doses of TBF (data not

260 shown). Therefore, 100 µg/mL was selected as the tested treatment concentration for further  
261 analysis in this study. These results indicate that high dose of glucose may evoke an imbalance  
262 of HepG2 redox status, and TBF protected HepG2 cells against the redox imbalance caused by  
263 high glucose.

#### 264 **Effect of TBF on Nrf2 and MAPKs under high glucose condition**

265 To continue the study of the protective effect of TBF against a high-glucose challenge, the  
266 levels of Nrf2 and MAPKs were evaluated. As shown in Fig. 3, high glucose significantly  
267 increased nuclear and total Nrf2 levels in comparison to control unchallenged HepG2 cells ( $p <$   
268  $0.05$ ). TBF alone also increased nuclear content and total levels of Nrf2, and showed higher  
269 levels of Nrf2 (nuclear) than high glucose-treated cells ( $p < 0.05$ ). Interestingly, the increased  
270 nuclear and total Nrf2 levels were unaltered when HepG2 cells were pre-treated with TBF as  
271 compared to glucose-challenged cells (Fig. 3). Moreover, phosphorylated levels of ERK, JNK  
272 and p38 increased significantly with high-glucose concentrations ( $p < 0.05$ , Fig. 4). TBF alone  
273 did not modify p-ERK and p-JNK levels, whereas decreased the p-p38 levels in comparison to  
274 the control cells. It was worth noting that pre-treatment with TBF significantly diminished the  
275 enhanced phosphorylated levels of all three MAPKs induced by high glucose ( $p < 0.05$ , Fig. 4).  
276 Total levels of ERK, JNK and p38 were not modified by any treatment. These results suggest  
277 that TBF can well modulate the high glucose-induced up-regulations of Nrf2 and MAPKs.

#### 278 **Effect of the MAPKs on TBF-induced change of Nrf2**

279 To further clarify the involvement of MAPKs in the modulation of Nrf2 levels induced by



280 TBF in high glucose-challenged cells, the effects of MAPKs selective inhibitors on these  
281 processes were assayed. First, HepG2 cells were pre-treated for 1 h with ERK and p38 inhibitors  
282 (PD98059 and SB203580), respectively, where both kinases have been demonstrated to be main  
283 regulators of Nrf2,<sup>13</sup> and then were treated with 100 µg/mL TBF for 24 h. In this regard, it has  
284 been reported that the inhibition of the two kinases may reduce nuclear and total levels of Nrf2  
285 caused by both cocoa flavonoids and high glucose in a non-pathological situation.<sup>16</sup> Next, it was  
286 examined whether ERK and p38 inhibition would also abolish the increase in the expression of  
287 Nrf2 provoked by TBF on high-glucose-challenged cells. As shown in Fig. 5, the blockage of  
288 ERK and p38 significantly reduced the nuclear and total levels of Nrf2 in comparison to TBF-  
289 and high glucose-treated cells ( $p < 0.05$ ), showing lower values than those of untreated and  
290 challenged controls. These results suggested that TBF-induced Nrf2 stimulation was mediated  
291 by ERK and p38, and the inhibition of both MAPKs similarly improved the protection induced  
292 by TBF.

#### 293 **Effect of the MAPKs on TBF-induced changes of ROS production, and GSH, GPx and GR** 294 **activities**

295 Following, the roles of MAPKs on the generation of ROS, and GSH, GPx, and GR activities  
296 were analyzed. As shown in Fig. 6, overproduction of ROS induced by high glucose was  
297 markedly avoided by TBF treatment, and the presence of MAPKs inhibitors further reduced the  
298 ROS production in the TBF pre-treated cells ( $p < 0.05$ ), but did not alter the levels of GSH.  
299 Additionally, ERK inhibitor increased GPx activity in cells pre-treated with TBF under high

300 glucose condition, whereas blockage of JNK and p38 did not alter this enzymatic activity (Fig.  
301 6). In addition, the blockage of p38 significantly increased GR activity in TBF pre-incubated  
302 cells under high glucose condition ( $p < 0.05$ ), but ERK and JNK inhibitors did not affect this  
303 enzymatic activity (Fig. 6). As a result, blockage of ERK and p38 improved the effects of TBF  
304 on GPx and GR activities in the high-glucose challenged cells, separately (Fig. 6). These results  
305 partly suggested that the protective effect of TBF could be enhanced by partly blocking MAPKs.

#### 306 **Effect of the MAPKs on TBF-induced changes of p-(Ser307)-IRS-1 and IRS-1 levels**

307 Since chronic high glucose treatment may induce the involvement of IRS-1 serine  
308 phosphorylation in the desensitization of insulin, and Ser307 is a key regulatory site among  
309 several potential serine phosphorylation sites of IRS-1, which is critical to the development of  
310 insulin resistance.<sup>37</sup> It has been reported that high-glucose provokes oxidative stress and insulin  
311 resistance, and MAPKs are involved in both processes,<sup>16</sup> so the effects of TBF and specific  
312 MAPKs inhibitor in insulin-induced Ser307 phosphorylation of IRS-1 and total IRS-1 levels  
313 under the high glucose concentration were analyzed. As shown in Fig. 7A and B, the level of  
314 insulin-stimulated Ser307 phosphorylation of IRS-1 was significantly increased with high  
315 glucose for 24 h, while total IRS-1 level was significantly decreased ( $p < 0.05$ ). However, TBF  
316 pre-treatment prevented the enhancement in p-(Ser307)-IRS-1 level and the decrease in total  
317 IRS-1 value induced by high glucose, achieving levels similar to the cells of treated with TBF  
318 alone ( $p < 0.05$ ). Additionally, the blockage of JNK in high glucose-challenged cells increased  
319 the reduction of total IRS-1 expression induced by the high-glucose concentration ( $p < 0.05$ ),

320 while did not significantly affect the p-(Ser307)-IRS-1 level. Furthermore, the inhibition of JNK  
321 in TBF-pretreated cells diminished the p-(Ser307)-IRS-1 to a value lower than the cells  
322 incubated with TBF alone. These data indicate that TBF reverses the activation of serine  
323 phosphorylation of IRS-1 induced by high glucose, and further JNK is involved in the  
324 stimulation of IRS-1 induced by TBF during insulin-resistance in HepG2 cells.

### 325 **Effect of the MAPKs on TBF-induced changes of glucose uptake**

326 As presented in Fig. 8, high glucose reduced the glucose uptake, whereas TBF alone  
327 increased the basal cell glucose uptake, and further pre-treatment of TBF was able to avoid the  
328 inhibited glucose uptake caused by the high concentration of glucose, showing high levels to  
329 those of TBF-treated cells. In addition, inhibition of all three MAPKs blocked the high-glucose  
330 induced reduction of glucose uptake in insulin-resistant cells, showing higher values than the  
331 untreated cells ( $p < 0.05$ ). Similarly, the blockage of MAPKs in TBF-pretreated cells completely  
332 prevented the diminished glucose uptake of the insulin resistant cells and evoked a higher  
333 beneficial effect than that of TBF alone ( $p < 0.05$ , Fig. 8). These results indicate that TBF  
334 protects the hepatic cell functions by improving the glucose uptake, and MAPKs inhibitors may  
335 improve the glucose uptake in insulin-resistant cells.

336

### 337 **Discussion**

338 Diabetes is strongly combined with increased oxidative stress, which is a consequence of  
339 either an increase of free radicals or reduction of antioxidant defenses.<sup>37</sup> Oxidative stress has

340 been proved as a result of long-term high glucose, and mediates diabetic complications in  
341 T2DM.<sup>49</sup> Additionally, the liver, the major modulator in maintaining blood glucose  
342 concentration, is particularly susceptible to toxic and oxidative insults.<sup>50</sup> However, numerous  
343 studies have demonstrated that tartary buckwheat flavonoids possess beneficial effects on  
344 antidiabetic effects in animals and humans,<sup>22</sup> and its main components, rutin and quercetin,  
345 which have a protective role against oxidative stress and insulin resistance,<sup>19,26,27,29</sup> may be  
346 proposed as potential therapeutic agents in the prevention or treatment of this disease. However,  
347 a clear molecular mechanism underlying these effects has not been established. In the present  
348 study, we firstly demonstrated that purified tartary buckwheat flavonoid fraction (TBF) could  
349 efficiently prevent the unbalance of cellular redox status which was provoked by high glucose  
350 via reducing ROS production and modulating the activities of antioxidant enzymes in human  
351 liver cells. Furthermore, TBF was also identified as an effective reagent in protecting the insulin  
352 resistance induced by high glucose to restore the impairment in glucose uptake which was first  
353 steps of the insulin transduction route (p-(Ser307)-IRS-1 and total IRS-1). The observed  
354 beneficial effects of TBF on redox balance and insulin resistance were accomplished by  
355 restraining signaling pathways related to stress namely MAPKs signal. Here, our data provide a  
356 new and detail molecular mechanism how tartary buckwheat can alleviate oxidative stress and  
357 insulin resistance under high glucose condition.

358 Direct evaluation of ROS yields is a good indicator of the oxidative damage to living cells.<sup>50</sup>  
359 Glutathione depletion reflects intracellular oxidation, whereas a balanced GSH concentration

360 could be expected to prepare the cell against a potential oxidative insult.<sup>36,51</sup> In the present study,  
361 we revealed that high glucose led to an overproduction of ROS, and as a direct consequence,  
362 oxidative damage to proteins was increased and GSH was depleted, which was consistent with  
363 the previously reports.<sup>16,52</sup> Changes in the activity of antioxidant enzymes can be considered as  
364 biomarkers of the antioxidant response.<sup>35,50</sup> CAT, GST and GPx are involved in eliminating  
365 peroxides providing an important cellular defence mechanism against oxidative damage,  
366 whereas GR recycles oxidized glutathione back to reduced glutathione.<sup>16,53</sup> Therefore, their  
367 activities are essential to the intracellular quenching of cell damaging peroxide species, and the  
368 effective recovery of the steady-state concentration of reduced glutathione can prevent the  
369 cytotoxicity of ROS overproduction.<sup>16,53</sup> Consistent with this, the significant increase in the  
370 activity of GPx and GR observed in our study clearly indicates a positive response of the cell  
371 defense system to face an oxidative insult. However, the GPx and GR activities in HepG2 cells  
372 treated with high concentrations of glucose were also increased, which evoked an imbalance of  
373 HepG2 redox status. These facts might reflect an adaptive mechanism in response to elevated  
374 oxidative stress during hyper-glycaemia.<sup>52</sup> Notably, GST activity remained unchanged in HepG2  
375 cells treated with high glucose, while the previous study reported that 30 mM glucose could  
376 decrease GST activity.<sup>16</sup> These facts may be related to a diminished hepatic enzymatic  
377 expression because of lower insulin stimulation during insulin resistance in T2DM,<sup>54</sup> and further  
378 investigations should be carried out. Furthermore, it has been shown that a glucose-induced  
379 increase in ROS generation and carbonyl content, and the decrease in GSH concentration were

380 prevented in cultured cells pre-treated with TBF in the present insulin-resistant model of HepG2  
381 cells. In this regard, it has been reported that both quercetin and rutin induce favorable changes  
382 in the antioxidant defense system of cultured HepG2 cells that may prevent or delay cellular  
383 oxidative stress.<sup>35,42</sup> In line with these, plant phenolics were reported to provide a parallel  
384 protection by increasing the activity of antioxidant enzymes.<sup>50,52</sup> Quercetin was reported to  
385 exhibit protective effect on human hepatoma cell line against oxidative stress induced by  
386 *tert*-butylhydroperoxide.<sup>55</sup> Numerous evidence suggests that rutin exhibits significant  
387 scavenging properties on oxygen radicals and plays a role in modulating oxidative stress by  
388 preventing ROS generation.<sup>56-58</sup> Consistent with these, our results revealed that pre-treatment of  
389 human HepG2 cells with TBF induced a significant increase in GPx and GR activities. Moreover,  
390 TBF effectively inhibited the alterations on antioxidant enzymatic activities caused by a high  
391 dose of glucose, suggesting that TBF exerted protective effects on the antioxidant defense  
392 system in a human HepG2 cells.

393 Nrf2 regulates the response to cellular stress and cell survival/proliferation, and plays a  
394 central role in the induction of phase II enzymes through its binding to the antioxidant response  
395 element after its nuclear translocation and phosphorylation.<sup>13</sup> In this regard, it has been  
396 described that both nuclear and total Nrf2 can be activated in response to high glucose treatment  
397 as an adaptive response to guard against oxidative and inflammatory cell damage,<sup>16</sup> where our  
398 result was in full agreement with this. Similarly, it has been shown that quercetin may activate  
399 Nrf2 by up-regulating the phosphorylation and translocation of Nrf2, and can modulate the

400 antioxidant defence, and these effects caused by quercetin seem to play an important role in the  
401 regulation of important glutathione-related enzymes.<sup>59,60</sup> In addition, rutin has been reported to  
402 significantly reduce oxidative stress and increase Nrf2 expression in injured livers of mice.<sup>61,62</sup>  
403 In line with this, it has been described that cocoa flavonoids stimulated Nrf2 with enhancing  
404 GPx and GR activities.<sup>16</sup> Consistent with these findings, we have found that TBF evokes an  
405 increase in GPx and GR activities in HepG2 cells in the present study, which correlates with  
406 Nrf2 activation. Although this finding deserves further investigation, the results above indicate  
407 that TBF-treated HepG2 cells are in favorable conditions to face the increasing generation of  
408 ROS induced by the high dose of glucose.

409 Oxidative stress-induced injury not only results from direct chemical interactions by altering  
410 cellular macromolecules, including DNA, proteins and lipids, but also implicates in profound  
411 alterations in signal transduction pathways.<sup>63</sup> Signaling cascades involving the MAPKs  
412 pathways are key mediators of stress signals and seem to be mainly responsible for protective  
413 responses and stress-dependent apoptosis reactions.<sup>18,64</sup> MAPKs are proved to be the upstream  
414 signals involved in Nrf2 activation, and would be activated in insulin-resistant HepG2 cells  
415 induced by hyperglycaemia.<sup>16</sup> Consistent with this, our study showed that phosphorylated levels  
416 of all three MAPKs were increased in insulin-resistant HepG2 cells. Additionally, pretreatment  
417 with TBF prevented the activation of MAPKs in hepatic cells treated with a high dose of  
418 glucose. In this line, it has been shown that the high glucose (15 mmol/L) induced  
419 phosphorylation of ERK and p38 could be significantly inhibited by rutin in human monocytic

420 THP-1 cells.<sup>65</sup> Moreover, quercetin inhibits lipid accumulation and obesity-induced  
421 inflammation by regulation of MAPK signaling factor expression in a dose-dependent manner in  
422 adipocytes and macrophages.<sup>66</sup>

423 MAPKs are also implicated in the up-regulation of antioxidant/detoxifiant enzymatic  
424 activities together with Nrf2 induction, which constitutes an important pathway to protect cells  
425 against oxidative damage.<sup>13</sup> As it has been reported that one of the major contributing  
426 mechanisms of Nrf2 activation by phenolic compounds is the phosphorylation of Nrf2 at  
427 specific serine and/or tyrosine residues via activation of upstream signaling pathways such as  
428 MAPKs.<sup>18</sup> In line with these, there have also been reported that the ERK and p38 inhibitors can  
429 decrease the nuclear and total levels of Nrf2 enhanced by the challenge with glucose or cocoa  
430 flavonoids, which shows lower values than the challenged hepatic cells.<sup>16</sup> In the present study,  
431 the selective inhibitor of ERK prevented the total accumulation of Nrf2 in TBF-pretreated  
432 HepG2 cells under high-glucose stress compared with TBF alone and high glucose challenged  
433 groups, and p38 inhibitor prevented the nuclear and total accumulations of Nrf2 in  
434 TBF-pretreated HepG2 cells under high-glucose stress. Additionally, overproduction of ROS  
435 activates the signaling cascades involving in MAPKs pathway.<sup>67</sup> In this regard, ROS generation  
436 has been described as a critical upstream mediator for the activation of JNKs, and the persistent  
437 activation of JNKs has been directly involved in the development of apoptosis in hepatocytes  
438 and non-hepatic cells.<sup>68</sup> Conversely, sustained activation of the ERKs has been shown to confer  
439 hepatocyte resistance to death.<sup>18</sup> In the present work, we firstly showed that TBF inhibited the



440 high glucose-induced increase of ROS, and this effect was improved in the presence of all three  
441 MAPKs inhibitors. Moreover, the GPx and GR activities restored by TBF in high  
442 glucose-challenged cells were modulated by the selective inhibitors of ERK and p38,  
443 respectively. These results indicate that the regulation of MAPK pathways by TBF may be  
444 implicated in Nrf2, and GPx and GR stimulation, and the kinase inhibitors may partly improve  
445 the protective effect of TBF. In this regard, it is reported that quercetin regulates GSH-related  
446 antioxidant/detoxifying enzymes and Nrf2 by targeting p38-MAPK,<sup>59</sup> and can prevent  
447 ethanol-induced hepatotoxicity via p38- and ERK1/2-mediated Nrf2 transcriptional activation.<sup>69</sup>  
448 However, other studies suggest that ERKs are implicated in the increased activities of GPx and  
449 GR in cocoa flavonoids-treated HepG2 cells.<sup>16</sup> In this case, it should be highlighted that further  
450 efforts are needed to elucidate the mechanisms of MAPKs involving in the protective effect of  
451 flavonoids on the high fructose induced oxidative stress. Altogether, these findings suggest that  
452 phosphorylation of all three MAPKs via ROS, glutathione-related enzymes and Nrf2 which  
453 probably decrease the oxidative stress, is involved in the protective mechanism of TBF against  
454 the oxidative stress induced by the hyperglycemia in HepG2 cells.

455 Studies have found that the lacking functions of insulin receptor substrate (IRS), a family of  
456 docking molecules connecting insulin receptor activation to essential downstream kinase  
457 cascades, may be the key molecular lesion signature of hepatic insulin resistance.<sup>37</sup> This defect  
458 appears to be a result of insulin-stimulated IRS-1 tyrosine phosphorylation resulting in the  
459 reduced IRS-1-associated phosphatidyl inositol 3 kinase activities.<sup>70</sup> Nevertheless, it was

460 demonstrated that serine phosphorylation of IRS-1 was involved in the desensitization of insulin  
461 by chronic high-glucose treatment,<sup>71</sup> and our study was consistent with this. However, we have  
462 found that TBF prevents the increase of p-(Ser307)-IRS-1 and the decrease of total IRS-1 level  
463 induced by high glucose exposure. Additionally, MAPKs have been identified as one of the  
464 important proteins in the development of insulin resistance by affecting glucose transporter  
465 expression and insulin signaling via modulation of total IRS-1 and phosphorylation of serine  
466 residues of IRS proteins.<sup>4,72</sup> It has been reported that ERK and JNK blockages can mediate the  
467 inhibition of p-(Ser636/639)-IRS-1 and p-(Ser307)-IRS-1, respectively, displaying negative  
468 regulators of hepatic insulin sensitivity,<sup>37</sup> whereas p38 seems to moderately affect p-(Ser)-IRS-1  
469 levels.<sup>73</sup> Consistent with this finding, the present study showed that the blockage of JNK could  
470 significantly decrease the levels of p-(Ser307)-IRS-1 in insulin-resistant TBF-treated cells. All  
471 these results suggest that TBF improves the cellular redox status and insulin resistance in high  
472 glucose-exposed HepG2 cells, and these protective effects of TBF are partly enhanced by the  
473 JNK inhibitor.

474 In the liver, GLUT2 maintains intracellular glucose in equilibrium with extracellular glucose,  
475 although this balance could be altered during insulin resistance.<sup>4,73</sup> It has demonstrated that  
476 GLUT2 levels and glucose uptake are decreased in HepG2 cells exposed to a high dose of  
477 glucose, and this may be reverted when pre-treated with natural antioxidant compounds.<sup>16</sup>  
478 Consistent with the above, the present study showed that TBF prevented the decrease of glucose  
479 uptake induced by high glucose in HepG2 cells, displaying a normalization of post-receptor

480 insulin signalling and a restoration of the hepatic insulin sensitivity. Furthermore, antioxidants  
481 have been found to protect the insulin-stimulated glucose transport against oxidative stress in  
482 cells,<sup>16</sup> and a role for ERK on the glucose uptake has been reported in hepatic cells.<sup>74</sup> It was also  
483 reported that rutin protected oxidative stress-induced insulin resistance in FL83B hepatocytes by  
484 improving 2-NBDG uptake through Akt phosphorylation and preventing PPAR $\gamma$  degradation,<sup>75</sup>  
485 and quercetin could ameliorate the hyperglycemic effect and oxidative stress parameters by  
486 inducing expression of GLUT4 via mRNA expression and translocation to the plasma  
487 membrane.<sup>3,76</sup> In the present study, inhibition of all three MAPKs improved the protective effect  
488 of TBF on glucose uptake. These results suggest that excess circulating glucose may be cleared  
489 by TBF and thereby protects individuals from glucotoxicity damages, and these studies deserve  
490 further investigations.

491 In conclusion, we firstly provide evidence that TBF may be bioactive natural substances with  
492 anti-diabetic effect as they can protect hepatic cells from oxidative stress induced by high  
493 glucose for enhancing the cellular antioxidant defence capacity. Furthermore, these beneficial  
494 effects of tartary buckwheat flavonoids on modulating the translocation of Nrf2 and alleviating  
495 this insulin resistance state might be mediated by MAPKs pathways. These findings suggest that  
496 TBF possesses protective effect against high glucose-induced oxidative stress and insulin  
497 resistance, which is considered as potential therapeutic strategies to preventing or delaying  
498 insulin-resistance disease like diabetes, and further experiments directed at the intimate  
499 mechanism of TBF are required.

500

501 **Acknowledgements**

502 This study was supported by grants from the National Natural Science Foundation of China  
503 (C31171678), and the Development program for Innovative Research Team of Shaanxi Normal  
504 University, China (GK201501006), as well as Science and Technology Innovation as a Whole  
505 Plan Projects of Shaanxi Province, China (2015KTCQ02-01).

506

507 **References**

- 508 1 S. Chinenye, A. E. Uloko, A. O. Ogbera, E. N. Ofoegbu, O. A. Fasanmade, A. A. Fasanmade  
509 and O. O. Ogbu, Profile of Nigerians with diabetes mellitus - Diabcare Nigeria study group  
510 (2008): results of a multicenter study, *Ind. J. Endocrinol. Metab.*, 2012, **16**, 558–564.
- 511 2 J. L. Evans, I. D. Goldfine, B. A. Maddux and G. M. Grodsky, Oxidative stress and  
512 stress-activated signaling pathways: a unifying hypothesis of type 2 diabetes, *Endocr. Rev.*,  
513 2002, **23**, 599–622.
- 514 3 M. M. Alam, D. Meerza and I. Naseem, Protective effect of quercetin on hyperglycemia,  
515 oxidative stress and DNA damage in alloxan induced type 2 diabetic mice, *Life Sci.*, 2014,  
516 **109**, 8–14.
- 517 4 P. J. Klover and R. A. Mooney, Hepatocytes: critical for glucose homeostasis, *Int. J.*  
518 *Biochem. Cell Biol.*, 2004, **36**, 753–758.
- 519 5 R. Dhanya, K. B. Arun, H. P. Syama, P. Nisha, A. Sundaresan, T. R. Santhosh Kumar and P.

- 520 Jayamurthy, Rutin and quercetin enhance glucose uptake in L6 myotubes under oxidative  
521 stress induced by tertiary butyl hydrogen peroxide, *Food Chem.*, 2014, **158**, 546–554.
- 522 6 J. Wang, H. Wang, P. Hao, L. Xue, S. Wei, Y. Zhang and Y. Chen, Inhibition of aldehyde  
523 dehydrogenase 2 by oxidative stress is associated with cardiac dysfunction in diabetic rats,  
524 *Mol. Med.*, 2011, **17**, 172-179.
- 525 7 G. Saravanan and P. Ponmurugan, Ameliorative potential of S-allyl cysteine on oxidative  
526 stress in STZ induced diabetic rats, *J. Chem. Biol. Interact.*, 2011, **189**, 100–106.
- 527 8 E. Ramiro-Puig, M. Urpí-Sardá, F. Pérez-Cano, A. Franch, C. Castellote, C.  
528 Andrés-Lacueva, M. Izquierdo-Pulido and M. Castell, Cocoa-enriched diet enhances  
529 antioxidant enzyme activity and modulates lymphocyte composition in thymus from young  
530 rats, *J. Agric. Food Chem.*, 2007, **55**, 6431–6438.
- 531 9 S. Ramos, Cancer chemoprevention and chemotherapy: dietary polyphenols and signalling  
532 pathways, *Mol. Nutr. Food Res.*, 2008, **52**, 507–526.
- 533 10 H. F. Zhang, L. J. Shi, G. Y. Song, Z. G. Cai, C. Wang and R. J. An, Protective effects of  
534 matrine against progression of high-fructose diet-induced steatohepatitis by enhancing  
535 antioxidant and anti-inflammatory defences involving Nrf2 translocation, *Food Chem.*  
536 *Toxicol.*, 2013, **55**, 70–77.
- 537 11 C. M. Liu, J. Q. Ma, W. R. Xie, S. S. Liu, Z. J. Feng, G. H. Zheng and A. M. Wang,  
538 Quercetin protects mouse liver against nickel-induced DNA methylation and inflammation  
539 associated with the Nrf2/HO-1 and p38/STAT1/NF- $\kappa$ B pathway, *Food Chem. Toxicol.*,

- 540 2015, **82**, 19–26.
- 541 12 A. B. Granado-Serrano, M. A. Martín, G. Haegeman, L. Goya, L. Bravo and S. Ramos,  
542 Epicatechin induces NF- $\kappa$ B, activator protein-1 (AP-1) and nuclear transcription factor  
543 erythroid 2p45-related factor-2 (Nrf2) via phosphatidylinositol-3-kinase/protein kinase B  
544 (PI3K/AKT) and extracellular regulated kinase (ERK) signalling in HepG2 cells, *Brit. J.*  
545 *Nutr.*, 2010, **103**, 168–179.
- 546 13 A. L. Egger, K. A. Gay and A. D. Mesecar, Molecular mechanisms of natural products in  
547 chemoprevention: induction of cytoprotective enzymes by Nrf2, *Mol. Nutr. Food Res.*,  
548 2008, **52**, S84–S94.
- 549 14 Y. Abe, S. Matsumoto, K. Kito and N. Ueda, Cloning and expression of a novel MAPKK-like  
550 protein kinase, lymphokine-activated killer T-cell-originated protein kinase, specifically  
551 expressed in the testis and activated lymphoid cells, *J. Biol. Chem.*, 2000, **275**, 1525–1531.
- 552 15 A. B. Granado-Serrano, M. A. Martín, M. I. Pulido, L. Goya, L. Bravo and S. Ramos,  
553 Molecular mechanisms of (-)-epicatechin and chlorogenic acid on the regulation of the  
554 apoptotic and survival/proliferation pathways in a human hepatoma cell line, *J. Agric. Food*  
555 *Chem.*, 2007, **55**, 2020–2027.
- 556 16 I. Cordero-Herrera, M. A. Martín, L. Goya and S. Ramos, Cocoa flavonoids protect hepatic  
557 cells against high-glucose-induced oxidative stress: Relevance of MAPKs, *Mol. Nutr. Food*  
558 *Res.*, 2015, **59**, 597–609.
- 559 17 A. Dey and J. Lakshmanan, The role of antioxidants and other agents in alleviating

- 560 hyperglycemia mediated oxidative stress and injury in liver, *Food Funct.*, 2013, **4**,  
561 1148–1184.
- 562 18 M. A. Martín, A. B. Serrano, S. Ramos, M. I. Pulido, L. Bravo and L. Goya, Cocoa  
563 flavonoids up-regulate antioxidant enzyme activity via the ERK1/2 pathway to protect  
564 against oxidative stress-induced apoptosis in HepG2 cells, *J. Nutr. Biochem.*, 2010, **21**,  
565 196–205.
- 566 19 P. V. A. Babu, D. Liu and E. R. Gilbert, Recent advances in understanding the anti-diabetic  
567 actions of dietary flavonoids, *J. Nutr. Biochem.*, 2013, **24**, 1777–1789.
- 568 20 P. Y. Qin, Q. Wang, F. Shan, Z. H. Hou and G. X. Ren, Nutritional composition and  
569 flavonoids content of flour from different buckwheat cultivars, *Int. J. Food Sci. Technol.*,  
570 2010, **45**, 951-958.
- 571 21 R. Karki, C. H. Park and D. W. Kim, Extract of buckwheat sprouts scavenges oxidation and  
572 inhibits pro-inflammatory mediators in lipopolysaccharide-stimulated macrophages  
573 (RAW264.7), *J. Integr. Med.*, 2013, **11**, 246-252.
- 574 22 H. W. Zhang, Y. H. Zhang, M. J. Lu, W. J. Tong and G. W. Cao, Comparison of  
575 hypertension, dyslipidaemia and hyperglycaemia between buckwheat seed-consuming and  
576 non-consuming Mongolian-Chinese populations in Inner Mongolia, China, *Clin. Exp.*  
577 *Pharmacol. P.*, 2007, **34**, 838–844.
- 578 23 N. Fabjan, J. Rode, I. J. Kosir, Z. Wang, Z. Zhang and I. Kreft, Tartary buckwheat  
579 (*Fagopyrum tataricum* Gaertn.) as a source of dietary rutin and quercitrin, *J. Agric. Food*

- 580 *Chem.*, 2003, **51**, 6452-6455.
- 581 24 Z. L. Zhang, M. L. Zhou, Y. Tang, F. L. Li, Y. X. Tang, J. R. Shao, W. T. Xue and Y. M. Wu,  
582 Bioactive compounds in functional buckwheat food, *Food Res. Int.*, 2012, **49**, 389–395.
- 583 25 M. Holasova, V. Fiedlerova, H. Smrcinova, M. Orsak, J. Lachman and S. Vavreinova,  
584 Buckwheat—the source of antioxidant activity in functional foods, *Food Res. Int.*, 2002, **35**,  
585 207–211.
- 586 26 N. T. Niture, A. A. Ansari and S. R. Naik, Anti-hyperglycemic activity of rutin in  
587 streptozotocin-induced diabetic rats: an effect mediated through cytokines, antioxidants  
588 and lipid biomarkers, *Indian J. Exp. Biol.*, 2014, **52**, 720-727.
- 589 27 C. C. Lee, B. H. Lee and Y. J. Lai, Antioxidation and antiglycation of *Fagopyrum tataricum*  
590 ethanol extract, *J. Food Sci. Technol.*, 2015, **52**, 1110-1116.
- 591 28 C. Y. Hsu, H. Y. Shih, Y. C. Chia, C. H. Lee, H. Ashida, Y. K. Lai and C. F. Weng, Rutin  
592 potentiates insulin receptor kinase to enhance insulin-dependent glucose transporter 4  
593 translocation, *Mol. Nutr. Food Res.*, 2014, **58**, 1168–1176.
- 594 29 E. P. Cai and J. K. Lin, Epigallocatechin gallate (EGCG) and rutin suppress the  
595 glucotoxicity through activating IRS2 and AMPK signaling in rat pancreatic  $\beta$  Cells, *J.*  
596 *Agric. Food Chem.*, 2009, **57**, 9817–9827.
- 597 30 D. Margina, D. Gradinaru, G. Manda, I. Neagoe and M. Ilie, Membranar effects exerted in  
598 vitro by polyphenols – quercetin, epigallocatechin gallate and curcumin – on HUVEC and  
599 Jurkat cells, relevant for diabetes mellitus, *Food Chem. Toxicol.*, 2013, **61**, 86–93.



- 600 31 M. Kanter, C. Aktas and M. Erbog, Protective effects of quercetin against apoptosis and  
601 oxidative stress in streptozotocin-induced diabetic rat testis, *Food Chem. Toxicol.*, 2012, **50**,  
602 719–725.
- 603 32 A. K. Shetty, R. Rashmia, M. G. R. Rajan, K. Sambaiah and P. V. Salimath, Antidiabetic  
604 influence of quercetin in streptozotocin-induced diabetic rats, *Nutr. Res.*, 2004, **24**, 373–381.
- 605 33 E. Youl, G. Bardy, R. Magous, G. Cros, F. Sejalon, A. Virsolvy, S. Richard, J. F.  
606 Quignard, R. Gross, P. Petit, D. Bataille and C. Oiry, Quercetin potentiates insulin secretion  
607 and protects INS-1 pancreatic  $\beta$ -cells against oxidative damage via the ERK1/2 pathway,  
608 *Brit. J. Pharmacol.*, 2010, **161**, 799–814.
- 609 34 Y. Y. Hu, Y. Zhao, L. Yuan and X. B. Yang, Protective Effects of Tartary Buckwheat  
610 Flavonoids on High TMAO Diet-Induced Vascular Dysfunction and Liver Injury in Mice,  
611 *Food Func.*, 2015, **6**, 3359–3372.
- 612 35 M. Alía, R. Mateos, S. Ramos, E. Lecumberri, L. Bravo and L. Goya, Influence of  
613 quercetin and rutin on growth and the antioxidant defense system in a human hepatoma cell  
614 line (HepG2), *Eur. J. Nutr.*, 2006, **45**, 19–28.
- 615 36 L. Goya, R. Mateos and L. Bravo, Effect of the olive oil phenol hydroxytyrosol on human  
616 hepatoma HepG2 cells. Protection against oxidative stress induced by  
617 *tert*-butylhydroperoxide, *Eur. J. Nutr.*, 2007, **46**, 70–78.
- 618 37 C. L. Lin and J. K. Lin, Epigallocatechin gallate (EGCG) attenuates high glucose-induced  
619 insulin signaling blockade in human hepG2 hepatoma cells, *Mol. Nutr. Food Res.*, 2008, **52**,

- 620 930–939.
- 621 38 I. Cordero-Herrera, M. A. Martín, L. Goya and S. Ramos, Cocoa flavonoids attenuate high  
622 glucose-induced insulin signalling blockade and modulate glucose uptake and production  
623 in human HepG2 cells, *Food Chem. Toxicol.*, 2014, **64**, 10–19.
- 624 39 T. Li, J. Zhu, L. Guo, X. L. Shi, Y. F. Liu, X. B. Yang, Differential effects of  
625 polyphenols-enriched extracts from hawthorn fruit peels and fleshs on cell cycle and  
626 apoptosis in human MCF-7 breast carcinoma cells, *Food Chem.*, 2013, **141**, 1008–101.
- 627 40 H. S. Zhang, M. Zhang, L. H. Yu, Y. Zhao, N. W. He, X. B. Yang, Antitumor activities of  
628 quercetin and quercetin-5',8-disulfonate in human colon and breast cancer cell lines, *Food*  
629 *Chem. Toxic.*, 2012, **50**, 1589-1599.
- 630 41 L. Yuan, Y. C. Wu, X. M. Ren, Q. Liu, J. Wang and X. Liu, Isoorientin attenuates  
631 lipopolysaccharide-induced pro-inflammatory responses through down-regulation of  
632 ROS-related MAPK/NF- $\kappa$ B signaling pathway in BV-2 microglia, *Mol. Cell Biochem.*,  
633 2014, **386**, 153–165.
- 634 42 L. Yuan, S. P. Wei, J. Wang and X. B. Liu, Isoorientin Induces Apoptosis and Autophagy  
635 Simultaneously by Reactive Oxygen Species (ROS)-Related p53, PI3K/Akt, JNK, and p38  
636 Signaling Pathways in HepG2 Cancer Cells, *J. Agric. Food Chem.*, 2014, **62**, 5390-5400.
- 637 43 P. Hissin and R. Hilf, A fluorimetric method for determination of oxidized and reduced  
638 glutathione in tissues, *Anal. Biochem.*, 1976, **74**, 214–226.
- 639 44 S. Richert, N. Wehr, E. Stadtman and R. Levine, Assessment of skin carbonyl content as a

- 640 non invasive measure of biological age, *Arch. Biochem. Biophys.*, 2002, **397**, 430–432.
- 641 45 J. T. Rotruck, A. L. Pope, H. E. Ganther, A. B. Swanson, D. G. Hafeman and W. G.  
642 Hoekstra, Selenium: biochemical role as a component of glutathione peroxidase, *Science*,  
643 1973, **179**, 588–590.
- 644 46 I. K. Smith, T. L. Vierheller and C. A. Thorne, Assay of glutathione reductase in crude  
645 tissue homogenates using 5,50-dithiobis (2-nitrobenzoic acid), *Anal. Biochem.*, 1988, **175**,  
646 408–413.
- 647 47 H. Aebi, Catalase. In: Bergmeyer, H.U. (Ed.), *Methods of Enzymatic Analysis*, Academic  
648 Press, New York, 1974, pp. 673–684.
- 649 48 W. H. Habig, M. J. Pabst and W. B. Jakoby, Glutathione S-transferases. The first enzymatic  
650 step in mercapturic acid formation, *J. Biol. Chem.*, 1974, **249**, 7130–7139.
- 651 49 T. Osawa and Y. Kato, Protective role of antioxidative food factors in oxidative stress  
652 caused by hyperglycemia, *Ann. N. Y. Acad. Sci.*, 2005, **1043**, 440–451.
- 653 50 M. A. Martin, S. Ramos, R. Mateos, A. B. Granado-Serrano, M. Izquierdo-Pulido, L. Bravo  
654 and L. Goya, Protection of human HepG2 cells against oxidative stress by cocoa phenolic  
655 extract, *J. Agric. Food Chem.*, 2008, **56**, 7765–7772.
- 656 51 M. C. Myhrstad, H. Carlsen, O. Nordstrom, R. Blomhoff and J. Ø. Moskaug, Flavonoids  
657 increase the intracellular glutathione level by transactivation of the  $\gamma$ -glutamylcysteine  
658 synthetase catalytical subunit promoter, *Free Radical Biol. Med.*, 2002, **32**, 386–393.
- 659 52 K. I. Seo, M. S. Choi, U. J. Jung, H. J. Kim, J. Yeo, S. M. Jeon and M. K. Lee, Effect of

- 660 curcumin supplementation on blood glucose, plasma insulin, and glucose homeostasis  
661 related enzyme activities in diabetic db/db mice, *Mol. Nutr. Food Res.*, 2008, **52**,  
662 995–1004.
- 663 53 R. Masella, R. D. Benedetto, R. Vari, C. Filesi and C. Giovannini, Novel mechanisms of  
664 natural antioxidant compounds in biological systems: involvement of glutathione and  
665 glutathione-related enzymes, *J. Nutr. Biochem.*, 2005, **16**, 577–586.
- 666 54 S. K. Kim and R. F. Novak, The role of intracellular signaling in insulin-mediated  
667 regulation of drug metabolizing enzyme gene and protein expression, *Pharmacol. Ther.*,  
668 2007, **113**, 88–120.
- 669 55 M. Alía, S. Ramos, R. Mateos, L. Bravo and L. Goya, Quercetin protects human hepatoma  
670 cell line (HepG2) against oxidative stress induced by *tert*-butyl hydroperoxide, *Toxicol.*  
671 *Appl. Pharmacol.*, 2006, **212**, 110–118.
- 672 56 Q. Li, Y. L. Qiu, M. Mao, J. Y. Lv, L. Zhang, S. Li, X. Li and X. Zheng, Antioxidant  
673 Mechanism of Rutin on Hypoxia-Induced Pulmonary Arterial Cell Proliferation, *Molecules*,  
674 2014, **19**, 19036-19049.
- 675 57 S. W. Wang, Y. J. Wang, Y. J. Su, W. W. Zhou, S. G. Yang, R. Zhang, M. Zhao, Y. N. Li, Z.  
676 P. Zhang, D. W. Zhan and R. T. Liu, Rutin inhibits  $\beta$ -amyloid aggregation and cytotoxicity,  
677 attenuates oxidative stress, and decreases the production of nitric oxide and  
678 proinflammatory cytokines, *NeuroToxicology*, 2012, **33**, 482–490.
- 679 58 C. H. Yeh, J. J. Yang, M. L. Yang, Y. C. Li and Y. H. Kuan, Rutin decreases

- 680 lipopolysaccharide-induced acute lung injury via inhibition of oxidative stress and the  
681 MAPK–NF- $\kappa$ B pathway, *Free Radical Bio. Med.*, 2014, **69**, 249–257.
- 682 59 A. B. Granado-Serrano, M. A. Martín, L. B. L. Goya and S. Ramos, Quercetin modulates  
683 Nrf2 and glutathione-related defenses in HepG2 cells: Involvement of p38, *Chem. Biol.*  
684 *Interact.*, 2012, **195**, 154–164.
- 685 60 P. Ramyaa and V. V. Padma, Ochratoxin-induced toxicity, oxidative stress and apoptosis  
686 ameliorated by quercetin – Modulation by Nrf2, *Food Chem. Toxicol.*, 2013, **62**, 205–216.
- 687 61 W. Arjumand, A. Seth and S. Sultana, Rutin attenuates cisplatin induced renal inflammation  
688 and apoptosis by reducing NF $\kappa$ B, TNF- $\alpha$  and caspase-3 expression in Wistar rats, *Food*  
689 *Chem. Toxicol.*, 2011, **49**, 2013–2021.
- 690 62 R. Domitrovć, H. Jakovac, V. V. Marchesi, S. Vladimir-Knežević, O. Cvijanović, Z.  
691 Tadić, Z. Romić and D. Rahelić, Differential hepatoprotective mechanisms of rutin and  
692 quercetin in CCl<sub>4</sub>-intoxicated BALB/cN mice, *Acta Pharmacol. Sin.*, 2012, **33**, 1260–1270.
- 693 63 M. J. Czaja, Induction and regulation of hepatocyte apoptosis by oxidative stress, *Antioxid.*  
694 *Redox Signal.*, 2002, **4**, 759–767.
- 695 64 H. J. Lee, C. J. Wang, H. C. Kuo, F. P. Chou, L. F. Jean and T. H. Tseng, Induction  
696 apoptosis of luteolin in human hepatoma HepG2 cells involving mitochondria translocation  
697 of Bax/Bak and activation of JNK, *Toxicol. Appl. Pharmacol.*, 2005, **203**, 124–31.
- 698 65 C. H. Wu, C. F. Wu, H. W. Huang, Y. C. Jao and G. C. Yen, Naturally occurring flavonoids  
699 attenuate high glucose-induced expression of proinflammatory cytokines in human

- 700 monocytic THP-1 cells, *Mol. Nutr. Food Res.*, 2009, **53**, 984–995.
- 701 66 M. J. Seo, Y. J. Lee, J. H. Hwang, K. J. Kim and B. Y. Lee, The inhibitory effects of  
702 quercetin on obesity and obesity-induced inflammation by regulation of MAPK signaling, *J.*  
703 *Nutr. Biochem.*, 2015, **26**, 1308–1316.
- 704 67 L. Pirola, A. M. Johnston and E. VanObberghen, Modulation of insulin action,  
705 *Diabetologia*, 2004, **47**, 170–184.
- 706 68 M. J. Czaja, The future of GI and liver research: editorial perspectives: III. JNK/AP-1  
707 regulation of hepatocyte death, *Am. J. Physiol. Gastr. L.*, 2003, **284**, 875–879.
- 708 69 P. Yao, A. Nussler, L. Liu, L. Hao, F. Song, A. Schirmeier and N. Nussler, Quercetin  
709 protects human hepatocytes from ethanol-derived oxidative stress by inducing heme  
710 oxygenase-1 via the MAPK/Nrf2 pathways, *J. Hepatol.*, 2007, **47**, 253–261.
- 711 70 K. F. Petersen and G. I. Shulman, Etiology of insulin resistance, *Am. J. Med.*, 2006, **119**,  
712 S10–S16.
- 713 71 V. Aguirre, E. D. Werner, J. Giraud, Y. H. Lee, S. E. Shoelson and M. F. White,  
714 Phosphorylation of Ser307 in insulin receptor substrate-1 blocks interactions with the  
715 insulin receptor and inhibits insulin action, *J. Biol. Chem.*, 2002, **277**, 1531–1537.
- 716 72 M. Fujishiro, Y. Gotoh, H. Katagiri, H. Sakoda, T. Ogihara, M. Anai, Y. Onishi, H. Ono, M.  
717 Abe, N. Shojima, Y. Fukushima, M. Kikuchi, Y. Oka and T. Asano, Three  
718 mitogen-activated protein kinases inhibit insulin signaling by different mechanisms in  
719 3T3-L1 adipocytes, *Mol. Endocrinol.*, 2003, **17**, 487–497.

- 720 73 K. Nakajima, K. Yamauchi, S. Shigematsu, S. Ikeo, M. Komatsu, T. Aizawa and K.  
721 Hashizume, Selective attenuation of metabolic branch of insulin receptor down-signaling  
722 by high glucose in a hepatoma cell line, HepG2 cells, *J. Biol. Chem.*, 2000, **275**,  
723 20880–20886.
- 724 74 H. N. Suh, Y. J. Lee and H. J. Han, Interleukin-6 promotes 2-deoxyglucose uptake through  
725 p44/42 MAPKs activation via Ca<sup>2+</sup>/PKC and EGF receptor in primary cultured chicken  
726 hepatocytes, *J. Cell. Physiol.*, 2009, **218**, 643–652.
- 727 75 C. C. Lee, W. H. Hsu, S. R. Shen, Y. H. Cheng and S. C. Wu, *Fagopyrum tataricum*  
728 (Buckwheat) Improved High-Glucose-Induced Insulin Resistance in Mouse Hepatocytes  
729 and Diabetes in Fructose-Rich Diet-Induced Mice, *Exp. Diabetes Res.*, 2012, **2012**,  
730 375673-375683.
- 731 76 M. L. Xu, J. J. Hu, W. W. Zhao, X. J. Gao, C. H. Jiang, K. Liu, B. L. Liu and F. Huang,  
732 Quercetin differently regulates insulin-mediated glucose transporter 4 translocation under  
733 basal and inflammatory conditions in adipocytes, *Mol. Nutr. Food Res.*, 2014, **58**, 931–941.

### Figure Captions

**Fig. 1** Effects of TBF on the increases of ROS generation and protein carbonyl content, and the decreases of GSH levels induced by high glucose in HepG2 cells. HepG2 cells were treated with 100 µg/mL TBF for 24 h and then were incubated with 30 mM glucose (Gluc) for another 24 h and further exposed to 100 nM (Ins) for 10 min. Data are expressed as percentage of controls. Values are means ± SD of 10 different samples per condition. Different letters over bars indicate statistically significant differences ( $p < 0.05$ ). Different styles of letters (normal, bold and italics) have been used for each parameter depicted within the same graph.

**Fig. 2** Effects of TBF on the activities of antioxidant/detoxifying enzymes GPx, GR, CAT and GST. HepG2 cells treated with 100 µg/mL TBF for 24 h were incubated with 30 mM glucose (Gluc) for additional 24 h and further exposed to 100 nM (Ins) for 10 min. Values are means ± SD of 10 different samples per condition. Different letters (normal, bold, italics and underlined) denote statistically significant differences,  $p < 0.05$ .

**Fig. 3** TBF induced the nuclear and total Nrf2 levels in HepG2 cells under high glucose condition. Cells were incubated with 100 µg/mL TBF for 24 h prior to 24-h glucose (Gluc) challenge and further exposed to 100 nM (Ins) for 10 min. (A) Bands of representative experiments. (B) Nrf2 values are evaluated by densitometric quantification. Values are means ± SD of 8 different samples per condition.  $\beta$ -actin or lamin B1 was used as an internal control.



Means without a common letter differ,  $p < 0.05$ .

**Fig. 4** Effects of TBF on the MAPK signaling pathway in HepG2 cells. Cells were treated with 100  $\mu\text{g/mL}$  TBF for 24 h and were later incubated with 30 mM glucose (Gluc) for another 24 h and further exposed to 100 nM (Ins) for 10 min. **(A)** Bands of representative experiments. **(B)** Densitometric quantification of p-ERK/ERK, p-JNK/JNK and p-p38/p38 ratios as a percentage to the control condition (means  $\pm$  SD,  $n = 8$ ).  $\beta$ -actin was used as an internal control. Different letters (normal, bold and italics) denote statistically significant differences,  $p < 0.05$ .

**Fig. 5** Effects of TBF and selective inhibitors of ERK (PD, PD98059) and p38 (SB, SB203580) on nuclear and total Nrf2 levels in HepG2 cells. The cells were incubated with 100  $\mu\text{g/mL}$  TBF for 24 h and then treated with 50  $\mu\text{M}$  PD or 10  $\mu\text{M}$  SB for 1 h prior to the 24-h glucose (Gluc) challenge and further exposed to 100 nM (Ins) for 10 min. **(A)** Bands of representative experiments. **(B)** Nrf2 values are evaluated by densitometric quantification as a percentage to the control condition (means  $\pm$  SD,  $n = 8$ ).  $\beta$ -actin or lamin B1 was used as an internal control. Means without a common letter differ,  $p < 0.05$ .

**Fig. 6** Effects of TBF and selective inhibitors of ERK (PD, PD98059), JNK (SP, SP600125) and p38 (SB, SB203580) on intracellular ROS production, and GPx, GR and GSH activities in HepG2 cells. The cells were incubated with 100  $\mu\text{g/mL}$  TBF for 24 h and were later treated with

50  $\mu$ M PD, 40  $\mu$ M SP, or 10  $\mu$ M SB for 1 h prior to 24-h glucose (Gluc) challenge, and further exposed to 100 nM (Ins) for 10 min. Intracellular ROS production and activities of GPx, GR and GSH are expressed as percentage of control as means  $\pm$  SD ( $n = 8$ ). Different letters (plain, bold, italics and underlined) denote statistically significant differences,  $p < 0.05$ .

**Fig. 7** Effects of TBF and selective inhibitors of JNK (SP, SP600125), ERK (PD, PD98059) and p38 (SB, SB203580) on p-(Ser307)-IRS-1 and total IRS-1 levels in HepG2 cells. The cells were incubated with 100  $\mu$ g/mL TBF for 24-h, followed by further treatment with 40  $\mu$ M SP, 50  $\mu$ M PD or 10  $\mu$ M SB for 1 h prior to 24-h glucose (Gluc) challenge and further exposed to 100 nM (Ins) for 10 min. **(A)** Bands of representative experiments. **(B)** Densitometric quantification of p-IRS1(Ser307) and total IRS-1 levels as a percentage to the control condition (means  $\pm$  SD,  $n = 8$ ).  $\beta$ -actin was used as an internal control. Different letters (plain, bold) denote statistically significant differences,  $p < 0.05$ .

**Fig. 8** Effects of TBF and selective inhibitors of JNK (SP, SP600125), ERK (PD, PD98059) and p38 (SB, SB203580) on glucose uptake in HepG2 cells. Glucose uptake expressed as percentage of control as means  $\pm$  SD ( $n = 8$ ). Different letters denote statistically significant differences,  $p < 0.05$ .

**Table 1**

Effects of TBF on cell viability and cell proliferation in HepG2 cells. Cell viability was expressed as relative percentage of control cells staining. Cell proliferation was calculated as percentage of the relative increase over the control values of BrdU incorporated into genomic DNA.

	Cell viability (percentage of viable cells)	Cell proliferation (percentage of controls)
Control	100.04 ± 4.97 <sup>a</sup>	100.65 ± 6.54 <sup>a</sup>
TBF (25 µg/mL)	100.80 ± 8.54 <sup>a</sup>	98.45 ± 7.72 <sup>a</sup>
TBF (50 µg/mL)	102.52 ± 6.89 <sup>a</sup>	102.39 ± 7.04 <sup>a</sup>
TBF (100 µg/mL)	104.25 ± 9.07 <sup>a</sup>	98.31 ± 10.49 <sup>a</sup>

Values are expressed as means ± SD of 10 samples per condition.

Means within a column with a common letter are equal,  $p < 0.05$ .

Figure 1

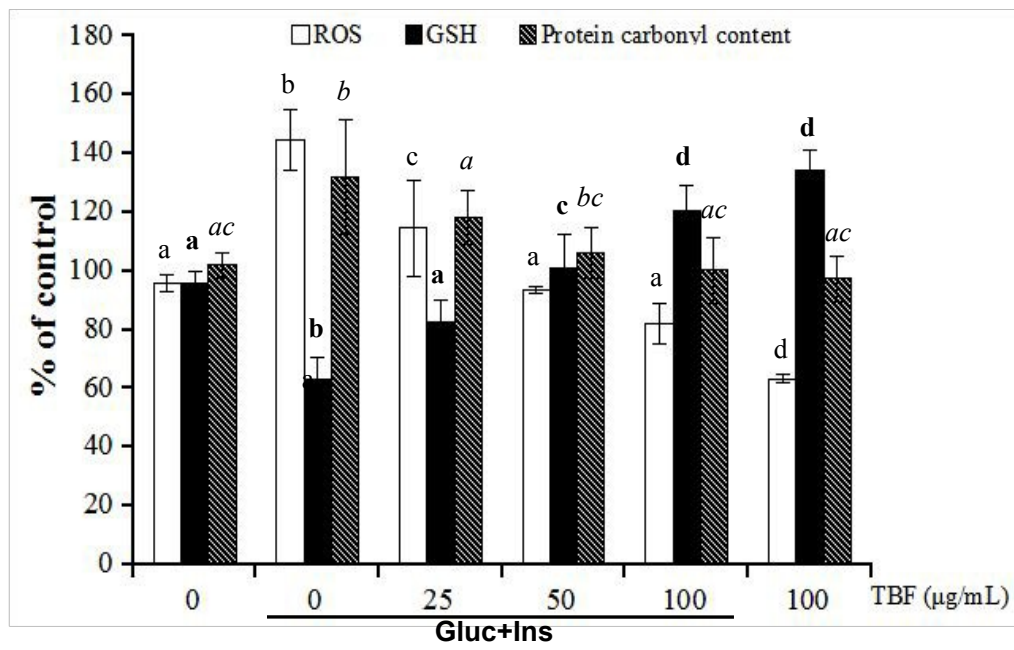


Figure 2

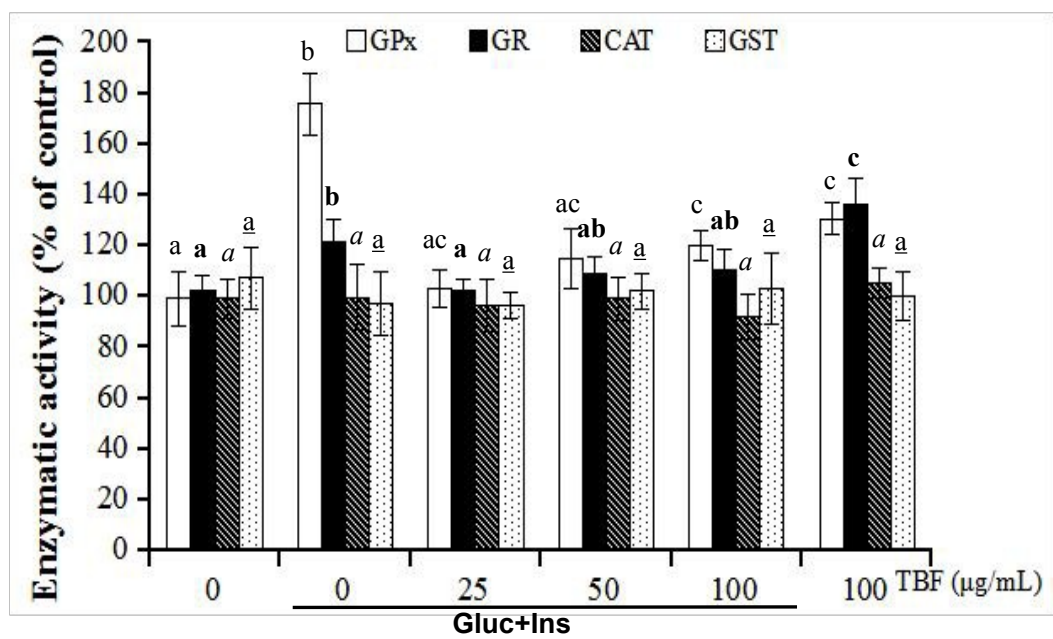
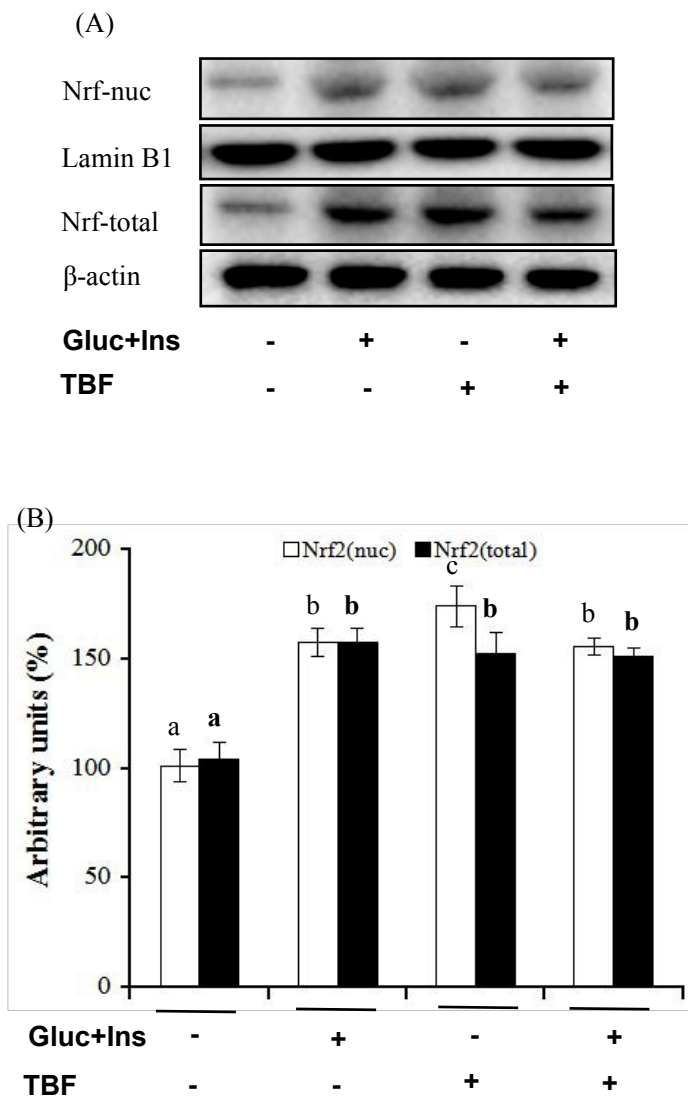


Figure 3



**Figure 4**

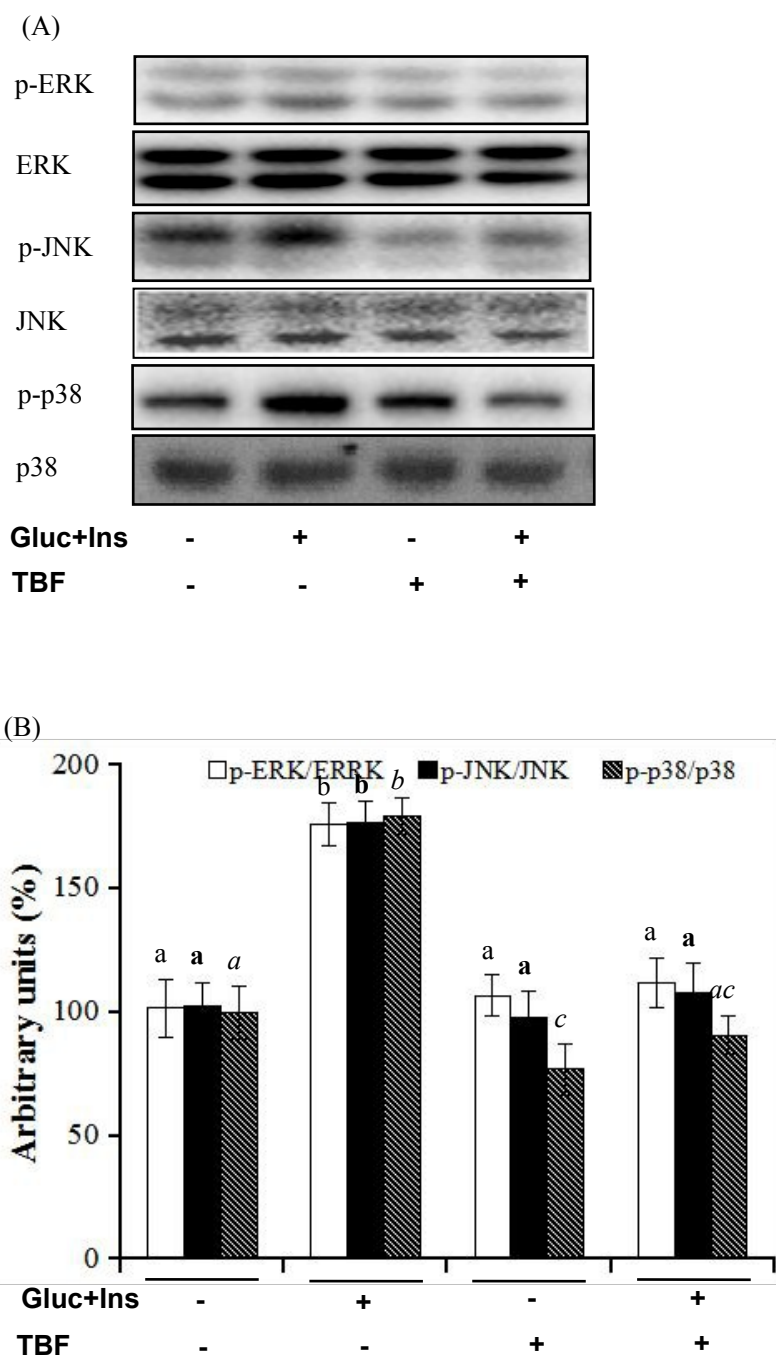


Figure 5

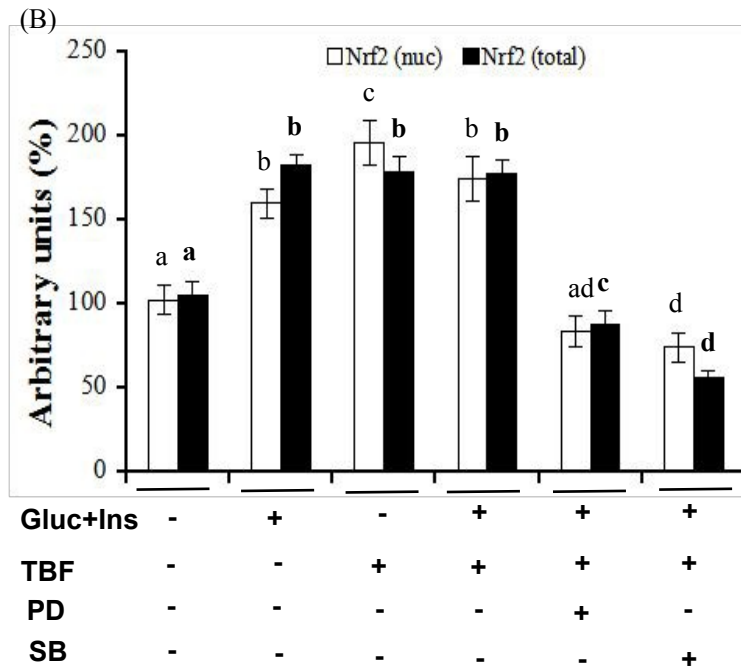
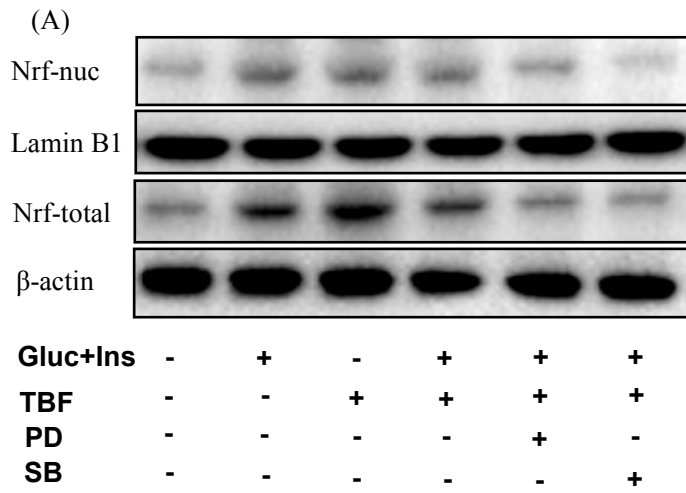




Figure 6

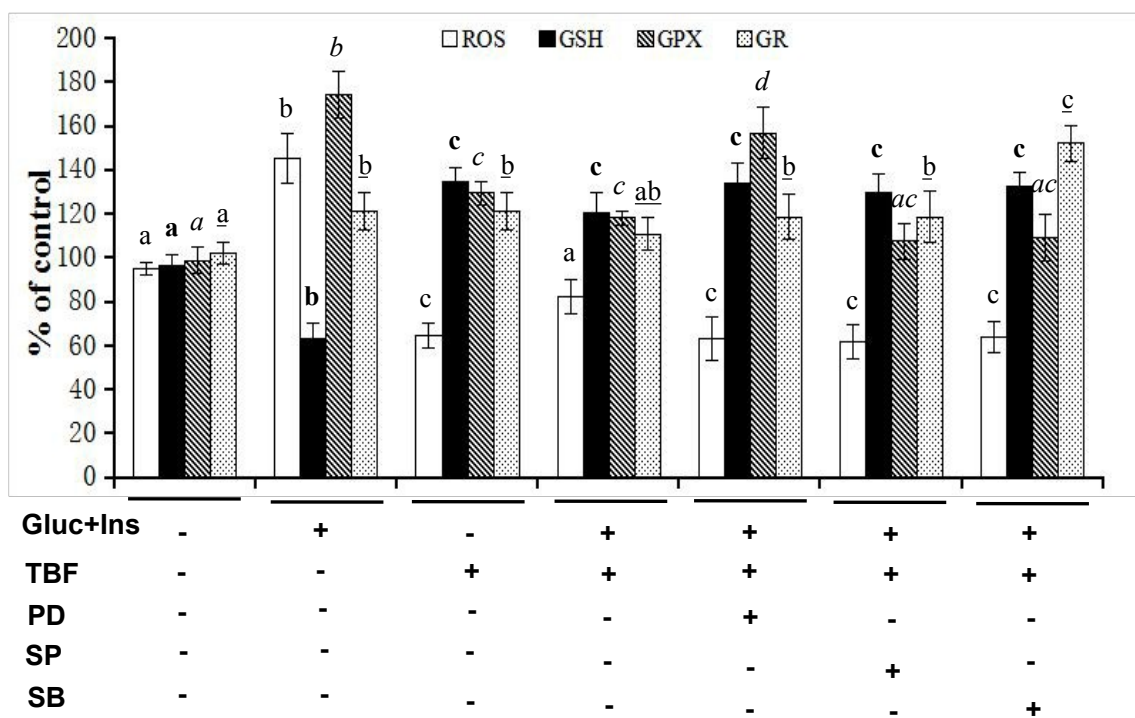


Figure 7

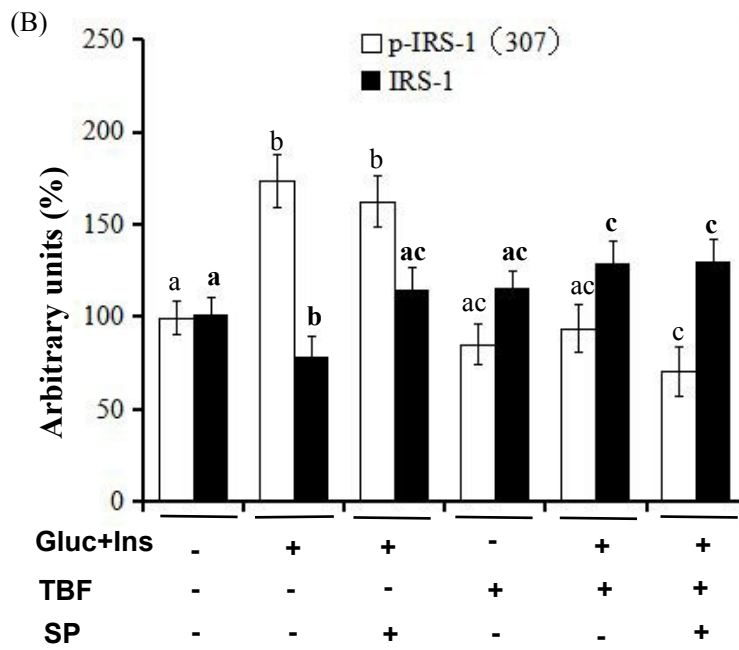
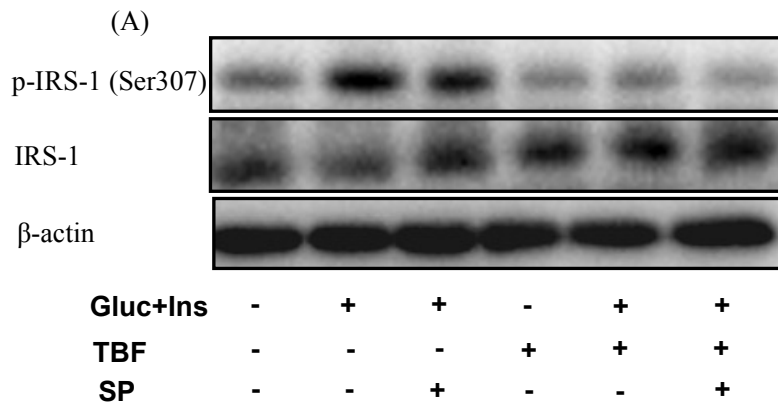


Figure 8

